


Article

Gradation Influence on Crack Resistance of Stress-Absorbing Membrane Interlayer

Ping Li ^{1,2}, Xuan Xiao ¹, Shuaituan Tian ³, Junbin Liu ⁴, Wenju Peng ^{1,5,*} , Bin Wang ⁶ and Shende Liu ¹

¹ School of Traffic & Transportation Engineering, Changsha University of Science & Technology, Changsha 410114, China; lipingchd@126.com (P.L.)

² Airport Engineering Research Center of CAAC, Beijing 100621, China

³ Beijing Super-Creative Technology Co., Ltd., Beijing 100621, China

⁴ Gezhouba Group Transportation Investment Co., Ltd., Wuhan 430030, China

⁵ School of Civil Engineering, Hubei Engineering University, Xiaogan 432000, China

⁶ Hunan Expressway Maintenance Engineering Co., Ltd., Changsha 410003, China

* Correspondence: pwj1112@foxmail.com

Abstract: Reflective cracking is a common distress of old pavement overlaid with an asphalt layer. The asphalt rubber stress-absorbing membrane interlayer can effectively mitigate and prevent reflective cracking. However, the existing test methods and evaluation indices for the crack resistance of the asphalt rubber stress-absorbing membrane interlayer are insufficient and unsystematic. They do not account for the significant effect of gradation parameters on the crack resistance in a comprehensive way. Therefore, this research aims to explore the impact of gradation parameters on the performance of the asphalt rubber stress-absorbing membrane interlayer. Based on the Chinese and U.S. standards, three kinds of 10 types of gradation were selected, forming a total of seven groups. The asphalt rubber stress-absorbing membrane interlayer was subjected to $-10\text{ }^{\circ}\text{C}$ and $15\text{ }^{\circ}\text{C}$ beam bending test, low-temperature semi-circular bend test, crack expansion semi-circular bend test, and overlay test to evaluate its cracking resistance. The correlation and influence law between the key sieve hole method, graded fractal method, and Bayley method parameters of different grades and beam bending test, low-temperature semi-circular bend test, crack expansion semi-circular bend test, and overlay test indexes were quantitatively analyzed by the coefficient of variation and Pearson correlation analysis method. The results showed that the performance of the mixtures with different gradation ranges varied significantly in different tests, as indicated by the maximum difference of 56.07% in stress absorption. This implied that gradation is a critical factor that affects the stress absorption performance of mixes. The different sensitivities of different tests to the parameters of the key sieve method, the graded fractal method, and the Bailey method indicated that the stress absorption performance was affected by a combination of factors. Therefore, in order to evaluate and optimize the stress absorption performance, it was necessary to comprehensively consider the interactions among the parameters of the key sieve method, the graded fractal method, and the Bailey method. The stress absorption performance included crack resistance and crack expansion resistance, which were inversely related and needed to be balanced and optimized during design. The $-10\text{ }^{\circ}\text{C}$ beam bending test and crack expansion semi-circular bend tests were more suitable test methods for evaluating stress absorption performance, and maximum flexural–tensile strain, strain energy density, fracture energy, and flexibility index were recommended as evaluation indicators. This research provides a reference for the optimization of the grading design of asphalt rubber stress-absorbing membrane interlayers, and provides test methods and indicators for the evaluation of crack resistance.



Citation: Li, P.; Xiao, X.; Tian, S.; Liu, J.; Peng, W.; Wang, B.; Liu, S. Gradation Influence on Crack Resistance of Stress-Absorbing Membrane Interlayer. *Appl. Sci.* **2023**, *13*, 11276. <https://doi.org/10.3390/app132011276>

Academic Editor: Jacek Tomków

Received: 5 September 2023

Revised: 9 October 2023

Accepted: 12 October 2023

Published: 13 October 2023



Copyright: © 2023 by the authors. Licensee MDPI, Basel, Switzerland. This article is an open access article distributed under the terms and conditions of the Creative Commons Attribution (CC BY) license (<https://creativecommons.org/licenses/by/4.0/>).

Keywords: crack resistance; gradation; reflective cracking; asphalt rubber stress-absorbing membrane interlayer

1. Introduction

For the maintenance of old roads or the reconstruction and upgrading of low-grade highways, the commonly adopted method is to overlay the asphalt pavement layer. Under the action of load and environment, the asphalt pavement layer will fill in the original old pavement joints and cracks at the occurrence of the stress concentration phenomenon, so that the asphalt pavement layer produces the bottom-up cracks-reflection cracks [1,2]. Reflective cracking can cause damage such as cracking and loosening, which significantly reduces the performance and service life of the pavement. To mitigate and prevent reflective cracking, stress-absorbing layer technology has been developed [3,4]. This technology involves adding a layer of material that can absorb the stress and strain caused by the movement of the old pavement, thus delaying or avoiding the formation of reflective cracks [5,6].

A stress-absorbing membrane interlayer is a type of interlayer material that is placed between the asphalt surface layer and the original old pavement or semi-rigid base. Its main function is to absorb or reduce the stress concentration that occurs at the joints or cracks of the old pavement, and to decrease the load stress and temperature stress at the bottom of the asphalt surface layer. This can slow down the initiation and expansion of reflective cracks, and effectively improve the service life of the asphalt surface layer [5,6]. The common materials for stress-absorbing layers are crumb-rubber-modified asphalt [7], geotextile [8], and smart composite [9]. Among them, crumb-rubber-modified asphalt has been widely used due to its excellent performance and sustainability [3].

Ogundipe [10,11] and Chen [7] examined the reflection cracking resistance performance of a stress-absorbing membrane interlayer (SAMI) under traffic load and found that the SAMI can significantly delay reflective cracking. Li [12] studied the reflection cracking resistance performance of six kinds of asphalt overlays by bending and shear tests. The results show that SAMPAVE (Stress Absorbing Mixtures Pavement), a stress absorbing mixture developed by Chang'an University, has excellent anti-cracking performance for fatigue. Pan [13] studied the crack resistance of warm mix rubber-modified asphalt mixture (WMRMA) by tensile stress restrained specimen test (TSRST) and finite element analysis method. The results show that WMRMA shows good low-temperature performance in the case of blending and compaction temperature fall of 30 °C, and it can delay the formation and extension of reflective cracks on the asphalt surface and prolong the service life of the asphalt surface. Baghel [14] developed a 3D finite element model to simulate the load response of inverted pavement with two types of interlayers: aggregate interlayer and stress-absorbing membrane interlayer. The results showed that the asphalt concrete layer of stress-absorbing membrane interlayer pavement experienced lower stress and strain levels than that of aggregate interlayer pavement. Yu [15] conducted the Hamburg wheel tracking test on four stress-absorbing interlayers, and the results showed that the asphalt-rubber sand concrete interlayer had the best reflection crack resistance performance. Asadi [16] conducted an experimental study on the influence of temperature, frequency, and geocomposite strength on the asphalt overlay cracking. The results revealed that temperature was the most significant factor in the reflective cracking rate. Shafabakhsh [17] examined the performance of natural zeolite and hydrated lime as additives for crumb-rubber-modified asphalt binder to prevent reflective cracking in composite pavements. The results show that both additives reduced the crack propagation rate, but natural zeolite was more effective than hydrated lime. Qiang [18] tested three kinds of warm mix rubber asphalt with different gradations and found that the gradation had a significant effect on the performance. Tran [19] conducted the notched semi-circular bending (SCB) test on seven different gradations of hot mix asphalt. The results show that the aggregate gradation has a significant correlation with the crack resistance of hot mix asphalt. Germann [20] invented the overlay test (OT). Zhou [21] improved the OT. Wang [22] tested the stress-absorption interlayer (SAI) with the waste tire rubber and amorphous poly alpha olefin complex modified asphalt binder and found that SAI has good fatigue resistance and reflection cracking resistance performance. It is considered that the number of cycles and the fracture property indexes

of the OT can effectively evaluate the reflection cracking resistance performance. Liu [23] used the ultimate bending strain and stress intensity factor as the evaluation indexes of the 5-type dense-graded stress-absorbing layer asphalt mixture to delay crack propagation. Zhou [24] reported that there are four main forms of asphalt pavement cracking: thermal, reflection, bottom-up fatigue, and top-down, and found that different tests reflect different forms of asphalt mixture cracking.

Previous studies have only conducted qualitative classification of gradation, without quantitatively evaluating its effect on stress absorption performance. Moreover, the existing research has considered a limited number of gradation types, which are not representative of different regions, and the recommended gradation ranges vary greatly among them. Therefore, it is necessary to further investigate the influence of gradation parameters on the performance of asphalt rubber stress-absorbing membrane interlayer (AR-SAMI). In addition, the cracking resistance of AR-SAMI is not adequately and systematically evaluated by the existing evaluation systems. Therefore, it is necessary to develop a comprehensive evaluation index system for AR-SAMI to provide a theoretical basis for its rational application.

The main objective of this research is to examine the influence and correlation of the key sieve method, the gradation fractal method, and the Bailey method parameters on the cracking resistance evaluation indices, and to propose suitable test methods and indices for evaluating the crack resistance performance of AR-SAMI. The beam bending test (BBT), low-temperature SCB (LT-SCB) test, crack expansion SCB (CE-SCB) test, and OT were conducted to measure the crack resistance of the AR-SAMI.

2. Materials and Methods

2.1. Crumb-Rubber-Modified Asphalt

The crumb-rubber-modified asphalt was prepared with 70#A grade base asphalt, 20% dosage of 30–80 mesh rubber powder, and stabilizer [25]. The stabilizer is produced by Guangxi Transportation Science and Technology Group Co., Ltd., Nanning, China. The properties of the rubber-modified asphalt are shown in Table 1.

Table 1. Properties of crumb-rubber-modified asphalt.

Physical Properties	Unit	Value	Technical Requirement [26]	Standard [27]
Penetration (25 °C, 100 g, 5 s)	0.1 mm	39.3	30~70	T 0604
Ductility (5 °C, 5 cm/min)	cm	11.6	>5	T 0605
Softening point	°C	75.5	>65	T 0606
Brookfield viscosity (180 °C)	Pa·s	2.51	2.0~5.0	T 0625
Elastic recovery rate (25 °C)	%	94.0	>60	T 0662

2.2. Aggregate

This study used limestone as both coarse and fine aggregates, and their main properties are shown in Table 2.

Table 2. Properties of aggregate.

Aggregate Types	Technical Index	Units	Value	Technical Requirement [28]	Standard [27]
Coarse aggregate	Crushing value	%	17	≤26	T 0316
	Apparent relative gravity	13.2 mm	2.705	≥2.60	T 0304
		9.5 mm	2.735		
		4.75 mm	2.63		
	Bulk specific gravity	13.2 mm	2.676	-	T 0304
9.5 mm		2.654			
4.75 mm		2.611			

Table 2. Cont.

Aggregate Types	Technical Index	Units	Value	Technical Requirement [28]	Standard [27]	
Coarse aggregate	Water absorption	13.2 mm	0.41	≤2.0	T 0304	
		9.5 mm	1.11			
		4.75 mm	0.27			
	Los Angeles abrasion loss	10–20 mm	15.6	≤30	T 0317	
		5–10 mm	20.1			
		3–5 mm	18.7			
Flat and elongated particles content	10–20 mm	13.2	≤15	T 0312		
	5–10 mm	10.9	≤15			
	3–5 mm	7.5	≤20			
Adhesional degree with aggregate		-	5	≥4	T 0616	
Fine aggregate	Bulk specific gravity		-	2.62	-	T 0304
	water absorption		%	0.27	-	T 0304
	Apparent specific gravity		-	2.622	≥2.50	T 0304
	Sand equivalent		%	69	≥60	T 0334
	Angularity (flow time method)		s	32.2	≥30	T 0345

2.3. Asphalt Mixture

2.3.1. Gradation

The mineral gradation of a stress-absorbing membrane interlayer can be mainly classified into two types: 5-type [29,30] and 10-type [28,31–38] gradation, with the latter being more prevalent. The 10-type gradation is mostly continuous, and all levels of gradation intersect and overlap with each other. The gradation curve analysis showed that the CAM [31] gradation had a gap at 0.15 mm sieve. The gradation of all levels had a significant difference in the passing rate of 4.75 mm sieve. The CAM, JTG F40-2004 [28], and DBJ/T13-147-2012 [38] had a higher passing rate of 4.75 mm sieve than the other gradations. Therefore, three types of type-10 gradations were classified as 10A, 10B, and 10C, as shown in Figure 1. The test gradation is shown in Figure 2.

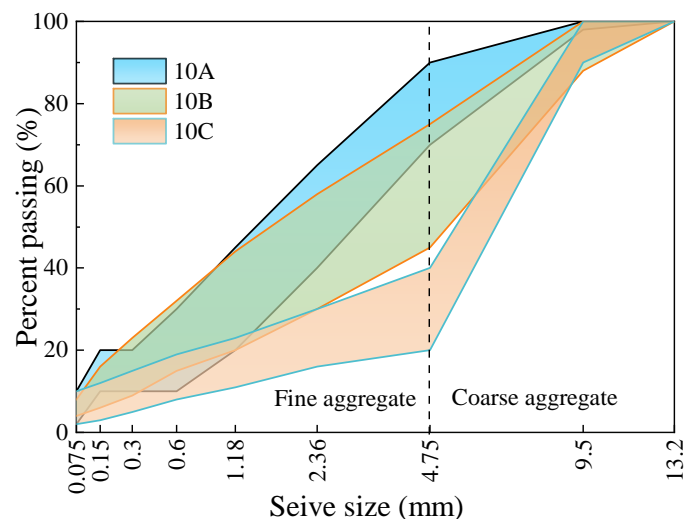


Figure 1. Classification of gradations of 10-type aggregate.

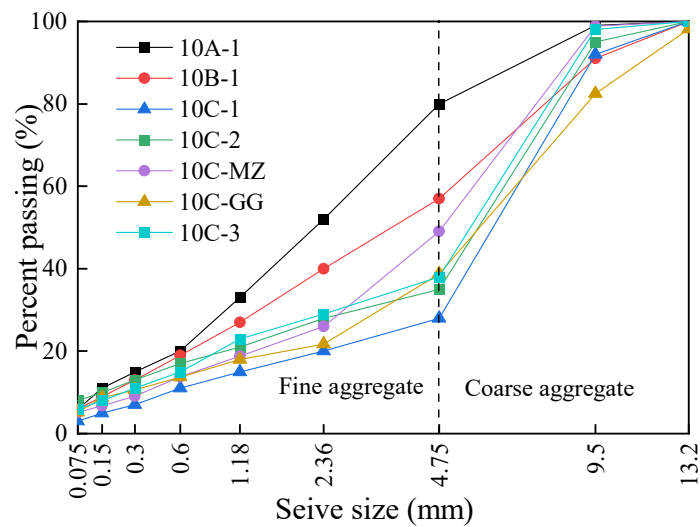


Figure 2. Gradation of AR-SAMI.

- (a) Referring to the gradation range of CAM, it was named 10A, and one gradation was selected and named 10A-1.
- (b) Referring to the gradation range of JTG F40-2004 and DBJ/T13-147-2012, it was named 10B, and one gradation was selected and named 10B-1.
- (c) Referring to the gradation range of DB45/T 1098-2014 [32], DB 36/T 744-2013 [33], DG/TJ08-2109-2012 [34], DB11/T 916-2012 [35], DB13/T 1013-2009 [36], and DB14/T 160-2015 [37], it was named 10C, and three gradations were selected and named 10C-1, 10C-2, 10C-3. Referring to the specific engineering gradation of Minzu (MZ) Avenue and Guigang (GG) Expressway, two gradations were selected and named 10C-MZ and 10C-GG.

To eliminate the influence of the change of air voids on the asphalt mixture, the Marshall design method was adopted. The optimum asphalt content was determined as the one corresponding to 2.5% design air voids. The volume parameters of the asphalt mixture are shown in Table 3.

Table 3. Asphalt mixture volume parameters.

Gradations Types	Optimal Asphalt–Aggregate Ratio/%	Theoretical Maximum Relative Density of Asphalt Mixture	Bulk Volume Relative Density of Asphalt Mixture	VV/%	VMA/%	VFA/%	Stability/kN	Flow Value/mm	FB	Asphalt Film Thickness/ μ m
10A-1	6.95	2.394	2.333	2.5	16.82	85.15	9.48	2.87	0.94	10.06
10B-1	6.10	2.425	2.364	2.5	15.11	83.41	8.65	2.76	1.08	9.70
10C-1	7.49	2.381	2.333	2.5	17.64	85.66	7.66	3.14	0.45	21.24
10C-2	6.55	2.410	2.343	2.5	15.93	84.38	7.81	3.33	1.35	9.71
10C-MZ	7.49	2.377	2.316	2.5	17.70	85.90	7.05	4.07	0.88	15.28
10C-GG	7.00	2.403	2.340	2.5	16.65	85.00	6.84	2.87	0.93	9.53
10C-3	6.46	2.409	2.350	2.5	15.78	84.18	7.84	3.78	1.02	11.51

2.3.2. Gradation Evaluation Methods

Gradation is an important factor that affects the performance of asphalt mixtures. It is of great significance to quantify the effect of gradation and evaluate the performance of mixtures using suitable evaluation parameters. The current methods for grading evaluation can be mainly classified into two categories: the key sieve method and the grading fractal method. The key sieve method evaluates the gradation by using the passing rates or ratios of certain key sieves or sieves in the mineral gradation. The grading fractal method evaluates the gradation by using the fractal theory to obtain the fractal dimension of composite gradation (D), the fractal dimension of coarse aggregate gradation (D_c), and the

fractal dimension of aggregate (D_f) of the gradation. The grading parameters used in this chapter are as follows:

- (a) Key sieve passing ratios. As shown in Figure 2, there is a large difference in the passing ratios at the 4.75 mm sieve among different gradations. According to JTG F40-2004 [28], the 10-type gradation uses the 2.36 mm sieve as the key sieve to distinguish between coarse and fine aggregates. The passing rates at the 4.75 mm and 2.36 mm sieves affect the voids in the mineral aggregate (VMA) and the air voids (VV) of the mixture, and VMA and VV affect the mixture properties. Therefore, $P_{4.75\text{mm}}$ and $P_{2.36\text{mm}}$ were selected as key sieve passing rates.
- (b) Key particle size aggregate content. The content of coarse aggregate above 2.36 mm affects the skeleton structure of the mixture and determines the initial voids in the mixture. Therefore, 4.75–9.5 mm and 2.36–4.75 mm were selected as key particle sizes.
- (c) The primary control sieve index (PCSI) [39]

$$PCSI = P_{PCS} - P_{PCS,MDL} \tag{1}$$

where $PCSI$ is the difference in percentage passing between the given gradation and the point on the maximum density line at the primary control sieve; P is the passage ratio of the corresponding sieve, %; d is the maximum nominal particle size, mm; the primary control sieve (PCS) is $0.22 \times d$, mm; $P_{PCS,MDL}$ is the passage ratio of the maximum density curve at PCS , taken as 47%, %.

- (d) Parameters of the Bailey method

$$CA = \frac{P_{D/2} - P_{PCS}}{100 - P_{D/2}} \tag{2}$$

$$FA_c = \frac{P_{SCS}}{P_{PCS}} \tag{3}$$

$$FA_f = \frac{P_{TCS}}{P_{SCS}} \tag{4}$$

where CA is the coarse aggregate ratio; FA_c is the fine aggregate coarse ratio; FA_f is the fine aggregate fine ratio; the secondary control sieve (SCS) is $0.22 \times PCS$; the third control sieve (TCS) is $0.22 \times TCS$.

- (e) Fractal dimension

$$D = 3 - k \tag{5}$$

where D is the mass fractal dimension; k is the slope of the fitting line obtained by linear regression in the double logarithmic coordinates of the sieve size and the passing rate. When only the part above 2.36 mm or below is taken, the gradation fractal dimensions D_c and D_f of coarse aggregate and fine aggregate can be calculated according to the fitting line, respectively.

The gradation parameters of the test gradations are shown in Table 4.

Table 4. Evaluation parameters of each gradation.

Gradation Types		10A-1	10B-1	10C-1	10C-2	10C-MZ	10C-GG	10C-3
Key sieve aggregate content (%)	4.75–9.5 mm	19	34	64	60	49.7	43.8	60
	2.36–4.75 mm	28	17	8	7	23.1	17	9
	$P_{4.75\text{mm}}$	80	57	28	35	49.1	38.7	38
	$P_{2.36\text{mm}}$	52	40	20	28	26	21.7	29
	PCSI	5	−7	−27	−19	−21	−25.3	−18
	CA	1.4	0.4	0.11	0.11	0.45	0.28	0.15
	FA_c	0.38	0.48	0.55	0.61	0.53	0.63	0.52
	FA_f	0.55	0.47	0.45	0.59	0.49	0.64	0.53
	D	2.44	2.45	2.35	2.52	2.4	2.46	2.45
	D_c	2.62	2.44	1.96	2.17	2.17	2.09	2.19
	D_f	2.42	2.46	2.42	2.64	2.52	2.57	2.52

2.4. Methods

The stress-absorbing performance can be evaluated from two aspects: crack resistance and crack expansion resistance. Crack resistance reflects the ability of the material to resist cracking under tensile stress, while crack expansion resistance reflects the ability of the material to prevent further crack expansion when cracks already exist. To evaluate these two aspects of the AR-SAMI performance, four test methods can be used: BBT, LT-SCB, CE-SCB, and OT. BBT is an important test to measure the tensile strength of the material, which can evaluate the crack resistance of the material under fatigue cracking and low-temperature shrinkage cracking conditions. The LT-SCB test can simulate the actual stress on the AR-SAMI under temperature stress and traffic load, which can evaluate the crack resistance of the material under low-temperature conditions. The CE-SCB test can evaluate the fracture characteristics of the asphalt mixture and obtain the crack propagation resistance of the mixture, which has a high correlation with the actual road performance of the AR-SAMI. The OT can simulate the basic characteristics of the reflective crack expansion in asphalt pavements. The classification of the stress absorption evaluated by these four test methods is shown in Table 5. Guangxi Province is situated in the southern part of China, between 20°54'–26°20' N. The 30-year average of the annual extreme minimum temperature in this region is −1.6 °C. To simulate the worst-case scenario, the minimum temperature of the test was set at −10 °C, while the room temperature was set at 15 °C. The test process is shown in Figure 3.

Table 5. Cracking patterns in response to the test methods.

Test Name	Crack Resistance	Crack Expansion Resistance
BBT	✓	
LT-SCB test	✓	
CE-SCB test		✓
OT		✓

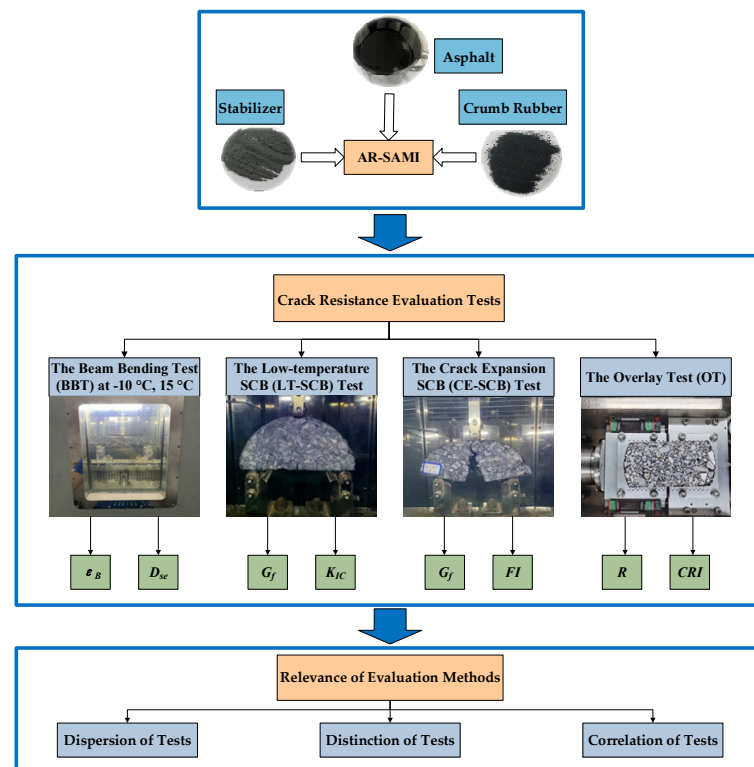


Figure 3. Experimental program to study the crack resistance performance of AR-SAMI.

2.4.1. BBT

The test was conducted according to JTG E20-2011 [27], using the universal material testing machine, under the conditions of test temperature $-10\text{ }^{\circ}\text{C}$, $15\text{ }^{\circ}\text{C}$, and loading rate 50 mm/min . There were three parallel test specimens for each group. The bending and tensile strength (R_B), bending tensile strain (ϵ_B), flexural modulus of strength (S_B), and strain energy density (D_{se}) were calculated according to the specifications.

2.4.2. LT-SCB Test

The process of preparing the LT-SCB test specimen is shown in Figure 4. The test was conducted according to AASHTO TP 105-13 [40], with an initial load of $1 \pm 0.1\text{ kN}$ and a loading speed of 0.6 mm/min to ensure the contact between the specimen and the loading device. After reaching the initial load, the load was continuously applied at a loading speed of 5.0 mm/min until the end of the test. The test was terminated when the first load below 0.5 kN was recorded or when the displacement transducer reached its maximum range. Four parallel specimens were tested for each group. The fracture energy (G_f) and fracture toughness (K_{IC}) were calculated according to the specifications.

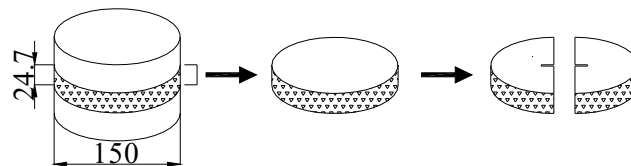


Figure 4. Preparation of LT-SCB test specimen.

2.4.3. CE-SCB Test

The process of preparing the CE-SCB test specimens is shown in Figure 5. The test was conducted according to EN 16697-44-2010 [41] and AASHTO TP 124-16 [42], with an initial stress of $0.1 \pm 0.01\text{ kN}$ applied to the specimens by a linear loading control system at a loading rate of 0.05 kN/s . After reaching the initial load of 0.1 kN , the test was carried out at a displacement rate of 50 mm/min by the linear loading control system. The test was terminated when the load dropped below 0.1 kN . Four parallel specimens were tested for each group. The G_f and flexibility index (FI) parameters were calculated according to the specifications.

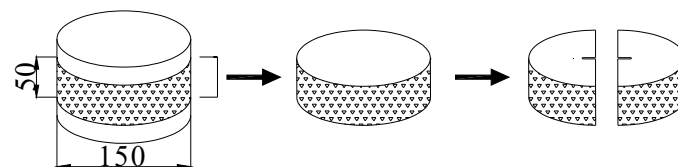


Figure 5. Preparation of CE-SCB test specimen.

2.4.4. OT

The process of preparing the OT specimens is shown in Figure 6. The test was conducted according to the TEX-248-F [43] protocol, with the following steps: the specimen was attached to the bottom plate of the apparatus using epoxy resin, and a weight of 2.268 kg was applied to the top and left to cure for 24 h . The test was carried out at a constant temperature of $25 \pm 0.5\text{ }^{\circ}\text{C}$ with a maximum constant displacement of 0.635 mm of the slider. The test was terminated when the maximum load decreased by 93% , or when the load reduction did not reach 93% within 1200 cycles. Three parallel specimens were tested for each group. The load loss rate (R) and the crack resistance index (CRI) were calculated according to the specifications.

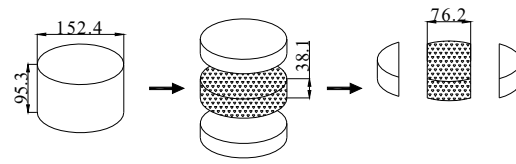


Figure 6. Preparation of OT specimen.

3. Results and Discussion

3.1. BBT

(a) The variation of R_B , ϵ_B , S_B , and D_{se} with gradation was inconsistent (as shown in Figure 7). As shown in Figure 8, there was a positive correlation between ϵ_B and D_{se} , while there was a negative correlation between ϵ_B and S_B . ϵ_B reflected the deformation resistance ability of the asphalt mixture, and D_{se} reflected the energy absorption ability of the material during the failure process. Both of them reflected the viscoelastic failure characteristics of the asphalt mixture, so they had a positive correlation. S_B was more suitable for the assessment of brittle failure, which was inconsistent with the failure mechanism of the asphalt mixture, so it had a negative correlation. In summary, ϵ_B and D_{se} were recommended as indicators for evaluating the performance of asphalt mixtures.

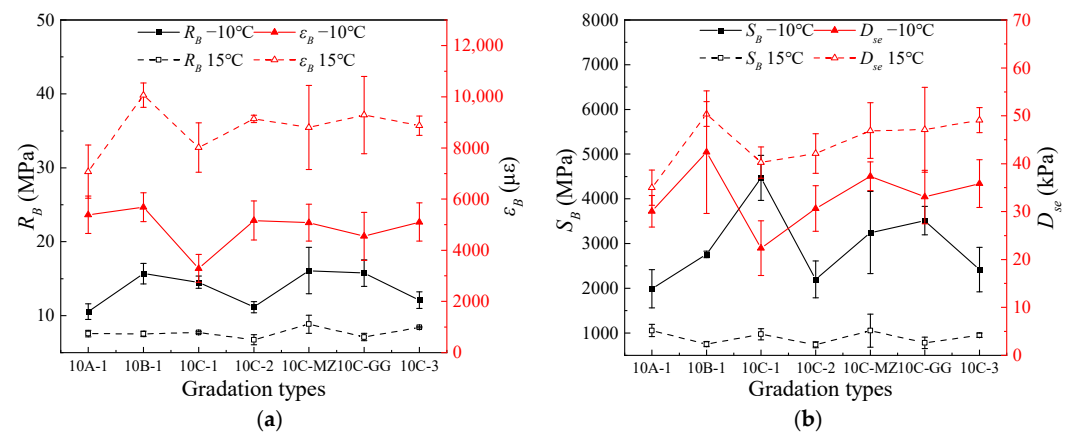


Figure 7. BBT results of AR-SAMI. (a) R_B and ϵ_B . (b) S_B and D_{se} .

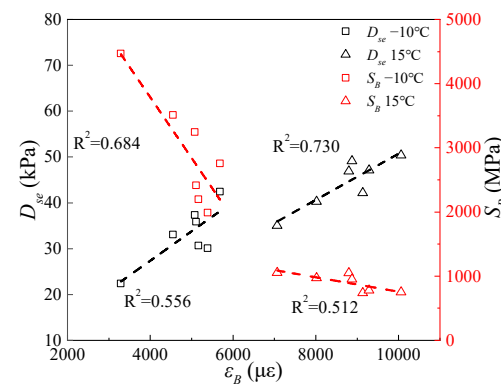


Figure 8. Correlation of evaluation indexes of BBT.

(b) The ϵ_B and D_{se} of different gradation mixtures were different. These values indicated the deformation and energy required for the failure of the asphalt mixtures under load. As shown in Figure 9, at -10°C , the maximum difference in ϵ_B was 2397.5 $\mu\epsilon$, and the maximum difference in D_{se} was 20.06 kPa. At 15°C , the maximum difference in ϵ_B was 2994.3 $\mu\epsilon$, and the maximum difference in D_{se} was 15.34 kPa. The 10B-1 had the highest values of ϵ_B and D_{se} at both temperatures, indicating that it had superior performance among the gradations.

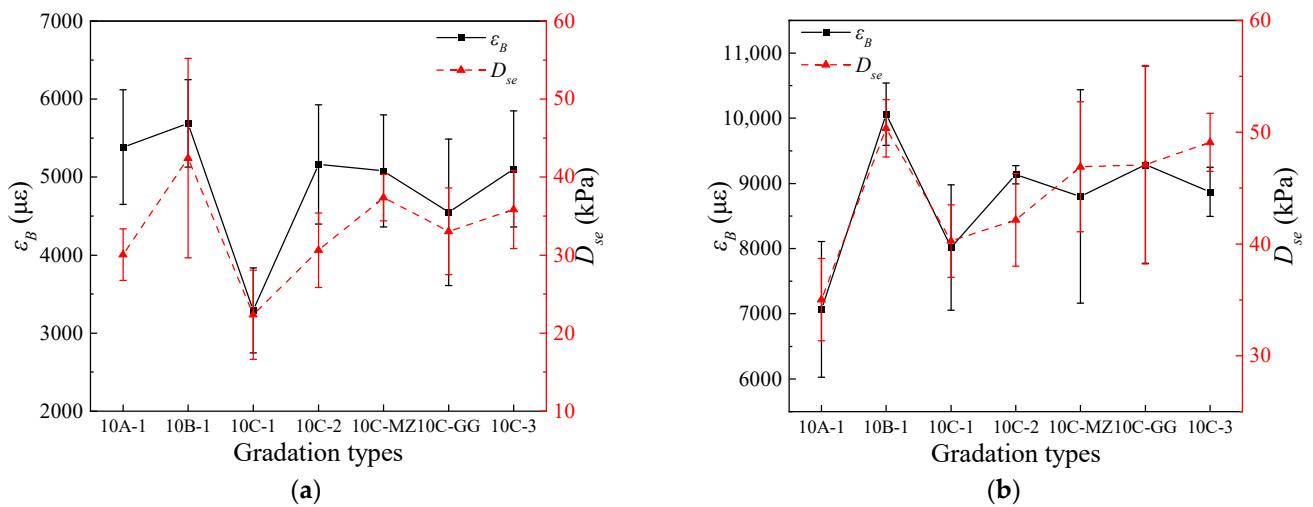


Figure 9. ϵ_B and D_{se} of different gradations. (a) ϵ_B and D_{se} at $-10\text{ }^\circ\text{C}$. (b) ϵ_B and D_{se} at $15\text{ }^\circ\text{C}$.

(c) There were differences in the correlation between the gradation parameters and the ϵ_B and D_{se} . The R^2 value of the linear regression of the same gradation parameter at different temperatures was also different. As shown in Figure 10, the $P_{4.75\text{mm}}$, $P_{2.36\text{mm}}$, $PCSI$, and D_c had strong correlations with ϵ_B and D_{se} at $-10\text{ }^\circ\text{C}$. At $15\text{ }^\circ\text{C}$, the $P_{4.75\text{mm}}$ had a better correlation with ϵ_B and D_{se} , while the $P_{2.36\text{mm}}$, $PCSI$, and D_c had a better correlation only with ϵ_B . For a more comprehensive analysis, the $P_{4.75\text{mm}}$, $P_{2.36\text{mm}}$, $PCSI$, and D_c were chosen to further analyze the effect of gradation.

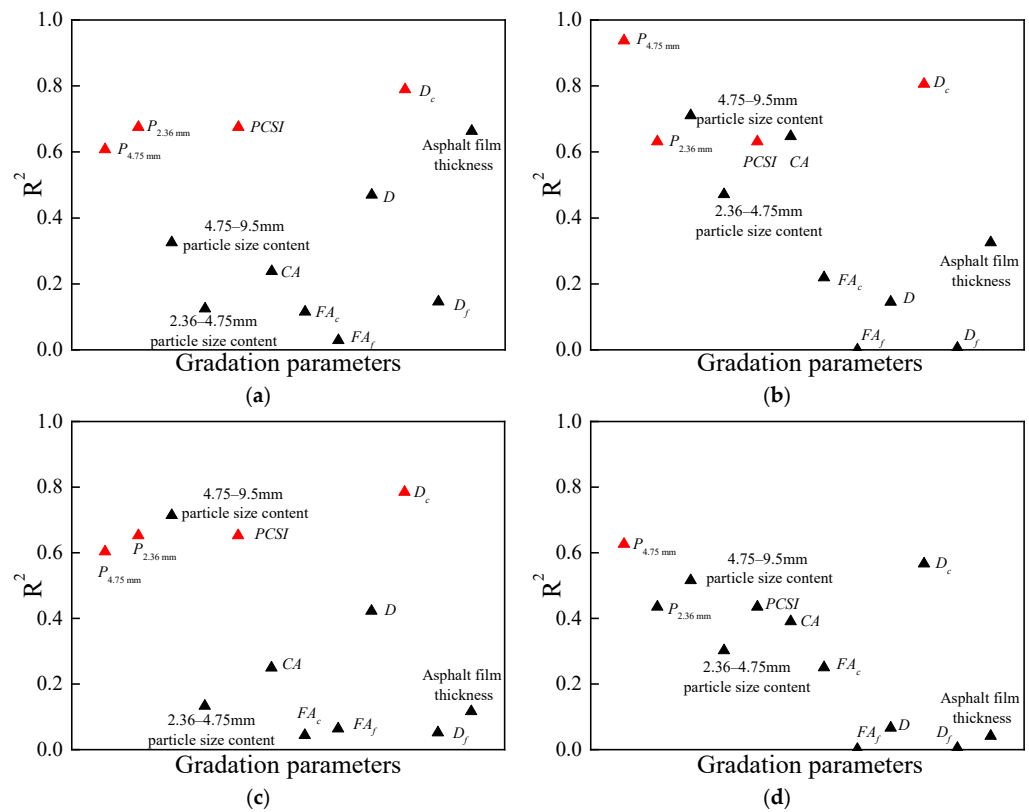


Figure 10. R^2 of gradation parameters fitting curve. (a) ϵ_B at $-10\text{ }^\circ\text{C}$. (b) D_{se} at $-10\text{ }^\circ\text{C}$. (c) ϵ_B at $15\text{ }^\circ\text{C}$. (d) D_{se} at $15\text{ }^\circ\text{C}$.

(d) As the $P_{4.75\text{mm}}$, $P_{2.36\text{mm}}$, $PCSI$, and D_c increased, ϵ_B and D_{se} of the mixture improved. As shown in Figure 11, the populated data points are for the 10A-1 gradation, which was not

fitted due to the differences in its relevant performance indexes from the other gradations. As the passing rate of sieves and $PCSI$ increased, the fine aggregate content in the mixture also increased, which enhanced the suspension effect of coarse aggregate in asphalt mortar. This caused a larger deformation during the bending failure process and consequently increased ϵ_B . The D_{se} of the asphalt mixture also increased with the bonding effect of asphalt mortar, which consumed more energy for the crack expansion during the bending failure. This index reflected that a more uniform gradation of asphalt mixture created a denser structure with smaller gaps between coarse aggregates. Therefore, in the gradation design, the D_c should be increased moderately to improve the bending resistance of the asphalt mixture. However, the D_c should not be excessive; otherwise, it will enhance the interference effect of finer aggregate and increase the porosity of the asphalt mixture, thus impairing its damage resistance. Based on this analysis, this paper recommends that the D_c should be controlled below 2.50.

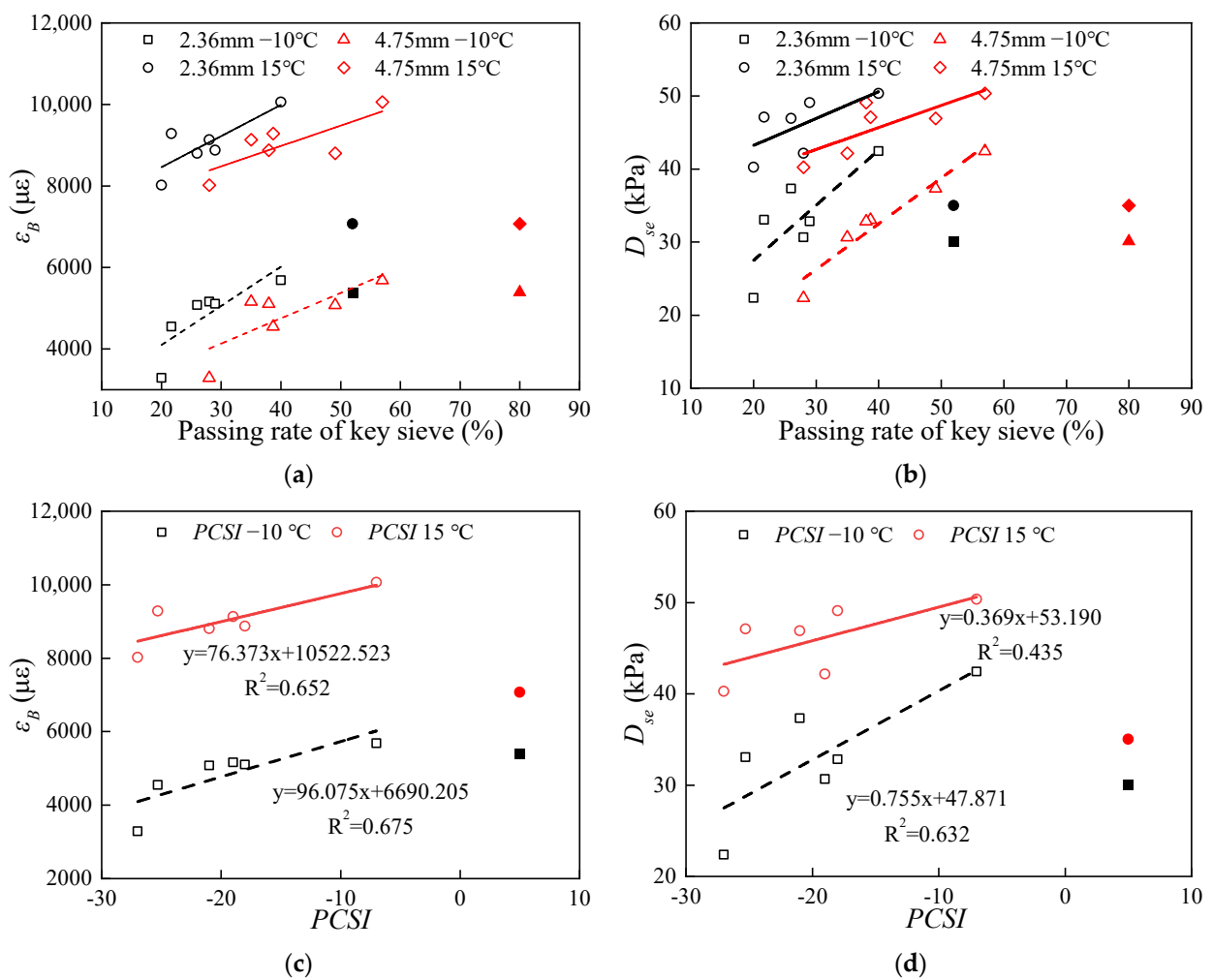


Figure 11. Cont.

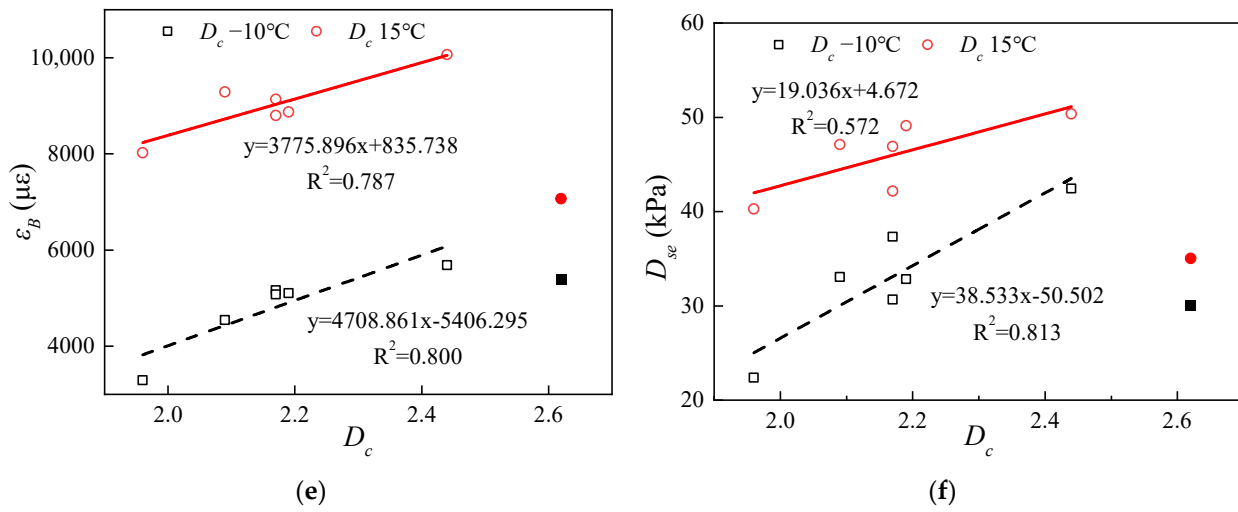


Figure 11. Correlation of gradation parameters with ϵ_B and D_{se} at -10 °C and 15 °C. (a) Passing rate of key sieve with ϵ_B . (b) Passing rate of key sieve with D_{se} . (c) PCSI with ϵ_B . (d) PCSI with D_{se} . (e) D_c with ϵ_B . (f) D_c with D_{se} .

3.2. LT-SCB Test

(a) Both the G_f and K_{IC} of the asphalt mixture were influenced by its gradation (as shown in Figure 12). These two parameters showed a similar trend and magnitude for different gradations. Furthermore, a strong linear correlation ($R^2 = 0.962$ and p -value < 0.01) between the G_f and K_{IC} was observed, as shown in Figure 13. The higher the values of G_f and K_{IC} , the better the performance and crack resistance of the asphalt mixture. Therefore, G_f and K_{IC} were recommended as indicators for evaluating the quality of the asphalt mixture.

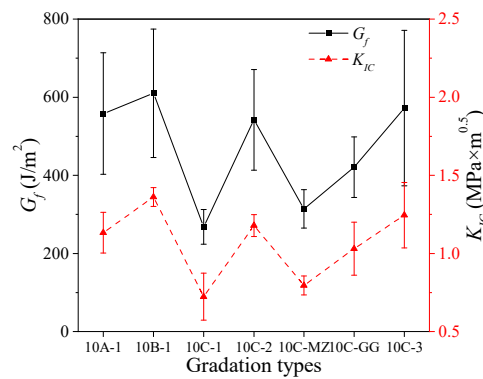


Figure 12. LT-SCB results of AR-SAMI.

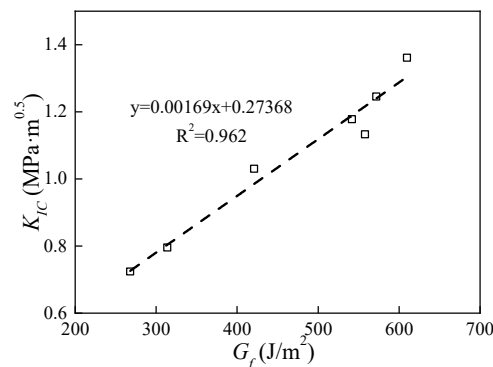


Figure 13. Correlation between G_f and K_{IC} .

(b) The G_f and K_{IC} of different gradation mixtures were different. The gradations of 10A-1 and 10B-1 had higher values of G_f and K_{IC} , indicating better resistance to load-induced damage. As shown in Figure 12, the maximum difference in G_f between the gradations was 342 J/m^2 , and the maximum difference in K_{IC} was $0.637 \text{ MPa}\cdot\text{m}^{0.5}$, with a maximum difference of 56.07%. The gradation of 10B-1 had the highest G_f and K_{IC} , while the gradations of 10C-1 and 10C-3 had the lowest values, suggesting that there might be considerable variability within the same gradation range.

(c) There were differences in the correlation between the grading parameters and the G_f and K_{IC} . As shown in Figure 14, the asphalt film thickness had the best correlation with G_f and K_{IC} , with R^2 values of 0.6873 and 0.6916, respectively. These values were both greater than 0.6, indicating a strong linear relationship. Therefore, the asphalt film thickness was selected as a parameter to further analyze the effect of gradation changes on the performance of the asphalt mixture.

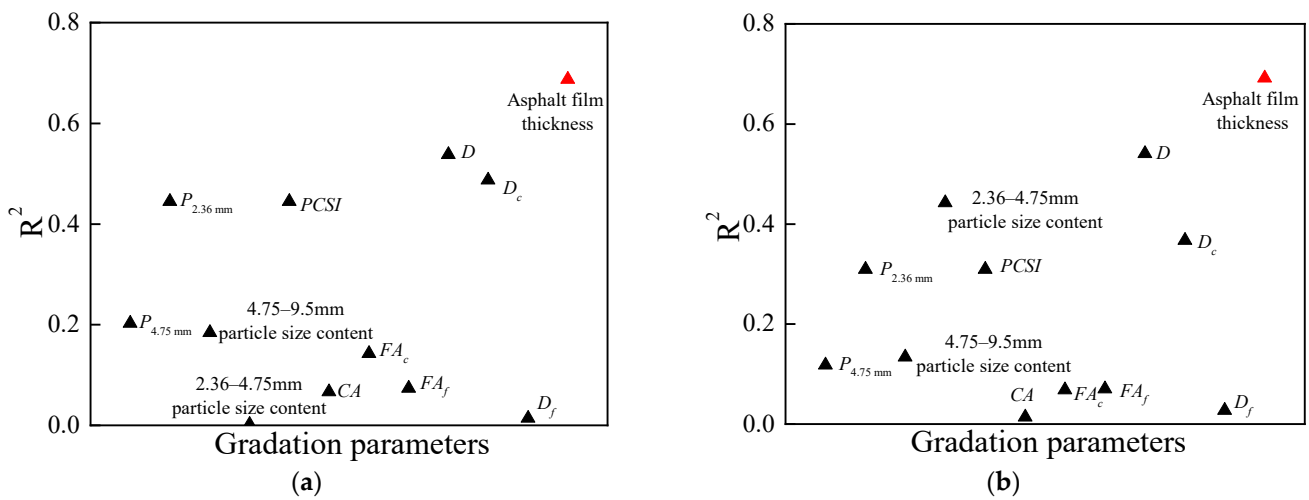


Figure 14. R^2 of gradation parameters fitting curve. (a) G_f . (b) K_{IC} .

(d) The G_f and K_{IC} of the asphalt mixture decreased as the asphalt film thickness increased (as shown in Figure 15). The reason for this was that when the asphalt film thickness reached a certain value, further increasing the thickness would result in some free asphalt inside the mixture, which made the mixture more susceptible to damage at low temperatures.

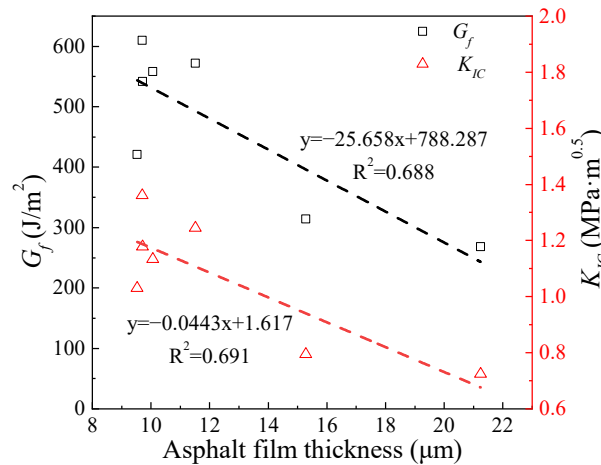


Figure 15. Correlation of the asphalt film thickness with G_f and K_{IC} .

3.3. CE-SCB Test

(a) The gradation of the asphalt mixture influenced both the G_f and FI (as shown in Figure 16). A good linear correlation between these two parameters was observed, with $R^2 = 0.843$ p -value < 0.01 (as shown in Figure 17). These results indicated that the G_f and FI of the asphalt mixture change in the same way with the gradation variation. Therefore, G_f and FI were recommended as evaluation indicators.

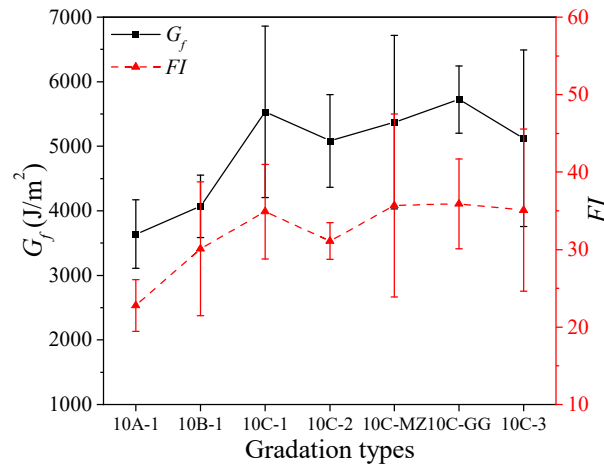


Figure 16. CE-SCB results of AR-SAMI.

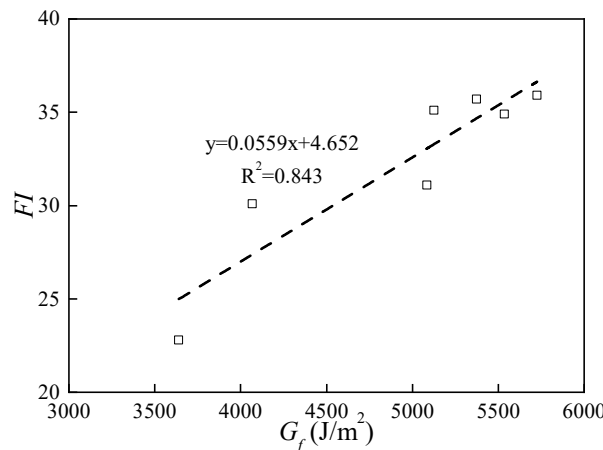


Figure 17. Correlation between G_f and FI .

(b) The G_f and FI varied among different gradations of the asphalt mixture, with the gradation of 10C having the highest values of these parameters. The G_f reflected the energy required for the asphalt mixture to develop and propagate cracks until failure, while the FI represented an intrinsic property of the material that characterizes the crack growth rate and the resistance to fatigue damage. As shown in Figure 16, the maximum difference in G_f between gradations was 2085 J/m², and the maximum difference in FI was 13.1, with a relative difference exceeding 30%. The gradation of 10A had the lowest G_f and FI , while all the 10C gradations had higher values of these parameters, indicating better resistance to load-induced damage.

(c) There were differences in the correlation between the grading parameters and the G_f and FI . As shown in Figure 18, the $P_{4.75mm}$ and $P_{2.36mm}$, $PCSI$, and D_c had the best correlation with G_f and FI , with R^2 values greater than 0.7. These values indicated a strong linear relationship. Therefore, these four parameters were selected to further analyze the effect of gradation changes on the performance of the asphalt mixture.

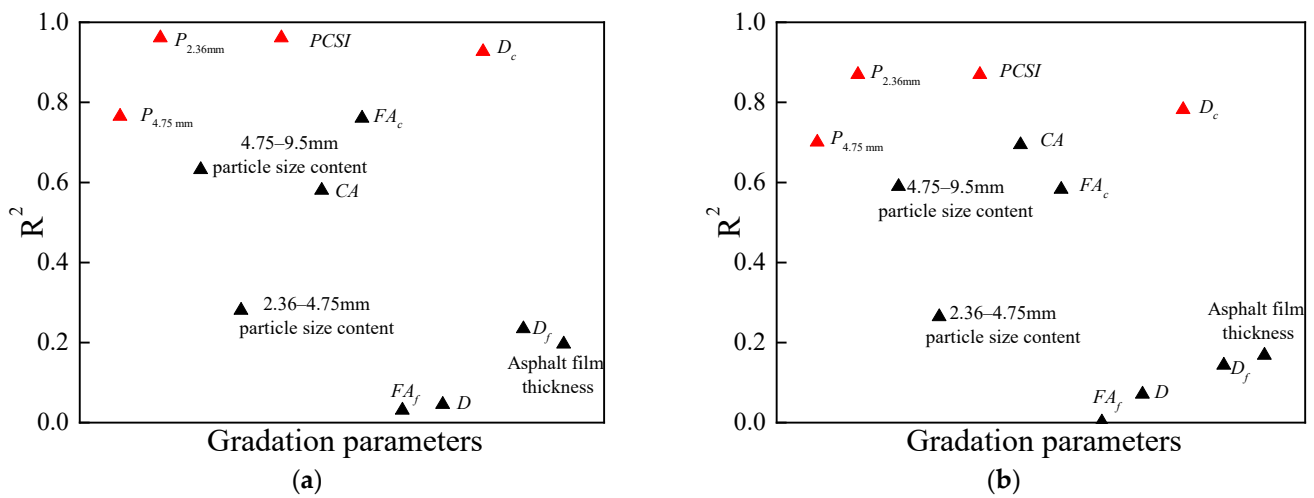


Figure 18. R^2 of gradation parameters fitting curve. (a) G_f . (b) FI .

(d) The G_f and FI of the asphalt mixture decreased with the increase of $P_{4.75mm}$, $P_{2.36mm}$, $PCSI$, and D_c , as shown in Figure 19. These parameters indicated that the gradation became finer, the fine aggregate content in the mixture increased, and the coarse aggregate was suspended in asphalt mortar. This reduced the resistance to crack expansion and accelerated the failure of the specimen. The increase of D_c also disrupted the coarse aggregate skeleton, which provided deformation resistance for the mixture. Therefore, the D_c value should be minimized in the gradation design.

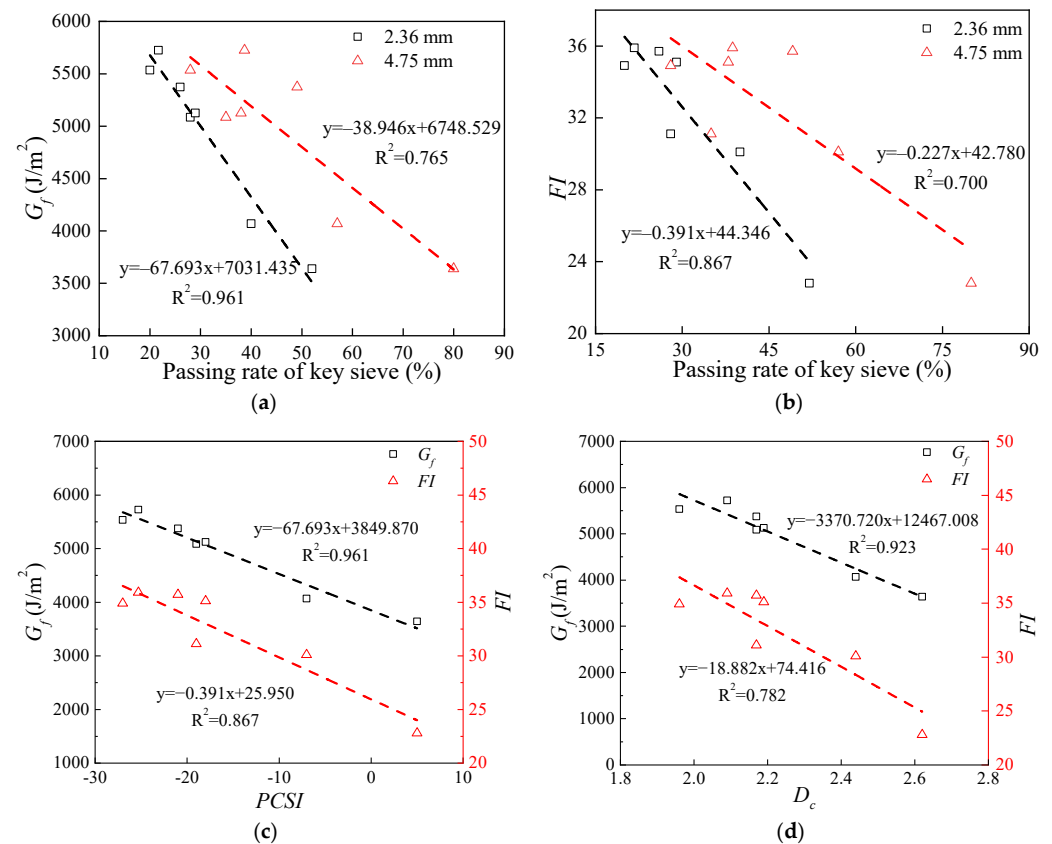


Figure 19. Correlation of gradation parameters with G_f and FI . (a) Passing rate of key sieve with G_f . (b) Passing rate of key sieve with FI . (c) $PCSI$ with G_f and FI . (d) D_c with G_f and FI .

(e) The coarse aggregate content has an effect on the crack resistance and crack expansion resistance. As shown in Figure 20, it can be seen that with the increase of coarse aggregate content, the peak load shows a trend of increasing and then decreasing, while the amount of deformation experienced to reach the peak load continues to increase. This indicates that an increase in the coarse aggregate content improves the aggregate skeleton strength and crack resistance. Excessive coarse aggregate content reduces the peak load of the asphalt mixture, but the amount of deformation experienced at the peak load continues to increase and the G_f does not show a significant decrease. After the peak load, the load decay of asphalt mixture with lower coarse aggregate content is faster, indicating that their resistance to crack expansion is poor. Combined with Figure 21, it can be found that the specimens with less crack expansion in the same gradation contain more and denser coarse aggregates, which indicates that the presence of coarse aggregates can effectively cause crack expansion resistance. The changes in crack extension between specimens of different gradation also show obvious differences, indicating that gradation has an important effect on crack expansion resistance.

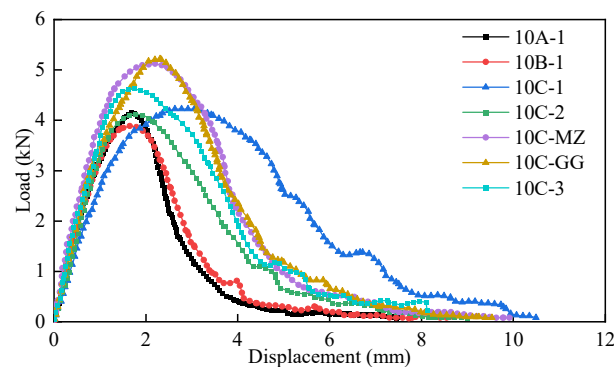


Figure 20. Load–displacement curve.

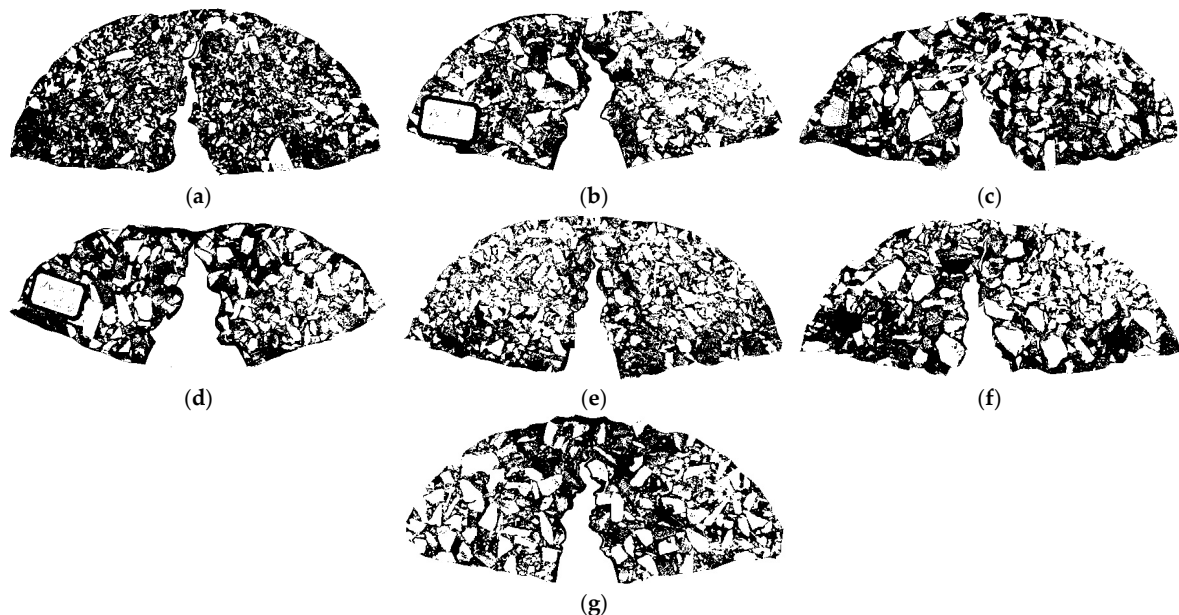


Figure 21. Binarization of SCB specimens. (a) 10A-1. (b) 10B-1. (c) 10C-1. (d) 10C-2. (e) 10C-MZ. (f) 10C-GG. (g) 10C-3.

3.4. OT

(a) The gradation of the asphalt mixture affected both the R and CRI (as shown in Figure 22). A good linear correlation between these two parameters was observed, with

$R^2 = 0.8906$ and p -value < 0.01 (as shown in Figure 23). These results suggest that the R and CRI of the asphalt mixture vary in the same way with the gradation changes. Therefore, R and CRI were recommended as evaluation indicators.

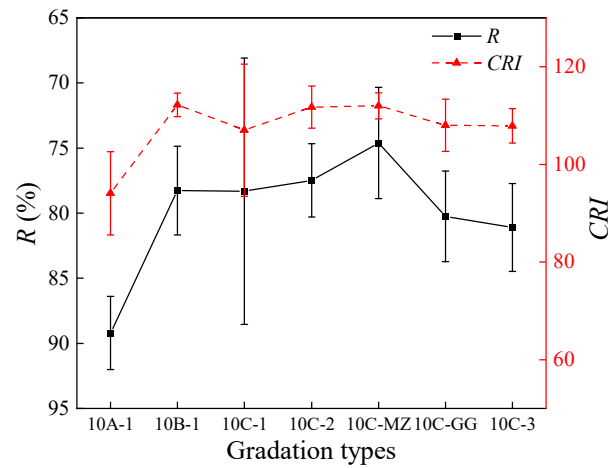


Figure 22. OT results of AR-SAMI.

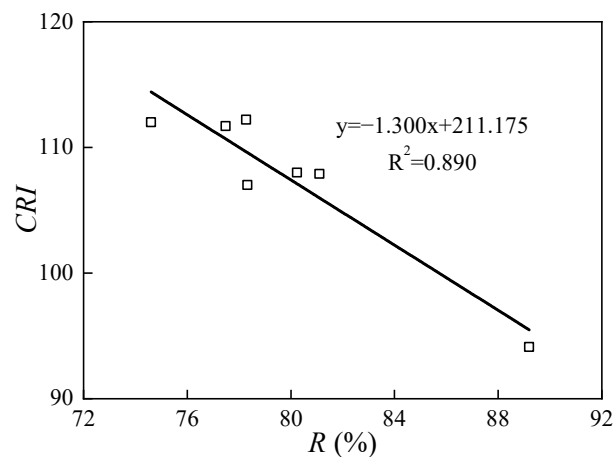


Figure 23. Correlation between R and CRI .

(b) The gradation of the asphalt mixture had an effect on the R and CRI . The R and CRI indicated the resistance of the asphalt mixture to damage under loading. As shown in Figure 22, the gradation range of 10A had the highest R and CRI , indicating the worst performance in terms of damage resistance. The gradation ranges of 10B and 10C had lower R and CRI , indicating better performance in terms of damage resistance. Among them, the gradation of 10A-1 had the highest R with a value of 14.59%, while the 10C-MZ gradation had the lowest value. The CRI had the lowest value for the gradation of 10A-1 and the highest value for the gradation of 10B-1 with a difference of 18.1%. Therefore, it can be concluded that the gradation range of 10A had unsatisfactory performance, while the gradation ranges of 10B and 10C had better performance.

(c) Correlation analysis of the gradation parameters with R and CRI showed that different gradation parameters affected the performance of the asphalt mixture to different degrees. As shown in Figure 24, the CA had the highest correlation coefficients with R and CRI , with values greater than 0.6. This indicated that CA was an important factor affecting the performance of the asphalt mixture. Therefore, CA was selected as the main parameter of gradation change to further explore its influence on the performance of the asphalt mixture.

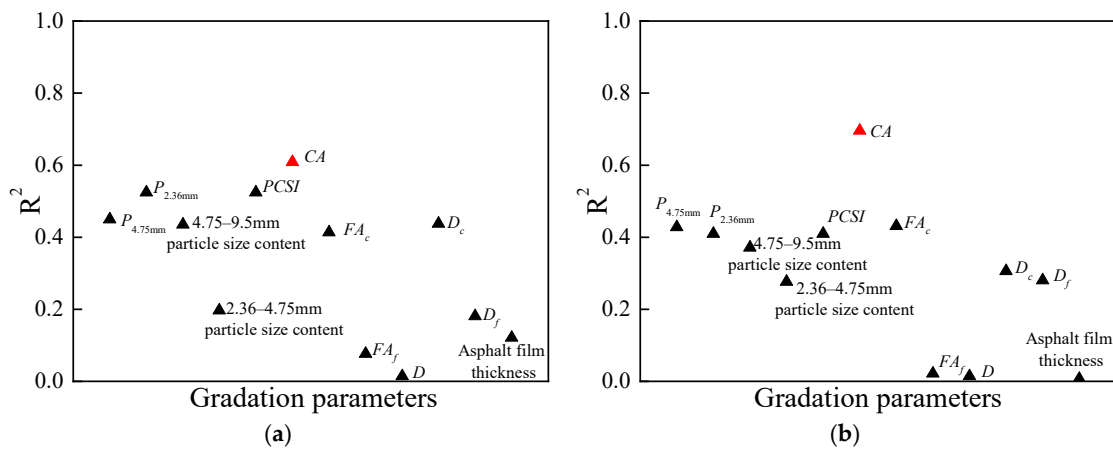


Figure 24. R^2 of gradation parameters fitting curve. (a) R . (b) CRI .

(d) The R of the asphalt mixture increased and the CRI decreased as the CA increased (as shown in Figure 25). When the CA increased, the content of 2.36 mm aggregate particles in the coarse aggregate fraction increased, which reduced the interlocking and stability of the coarse aggregate skeleton and disrupted the dense structure of the asphalt mixture. As a result, the cracks encountered less resistance and propagated faster during the OT, leading to lower performance and higher damage to the asphalt mixture.

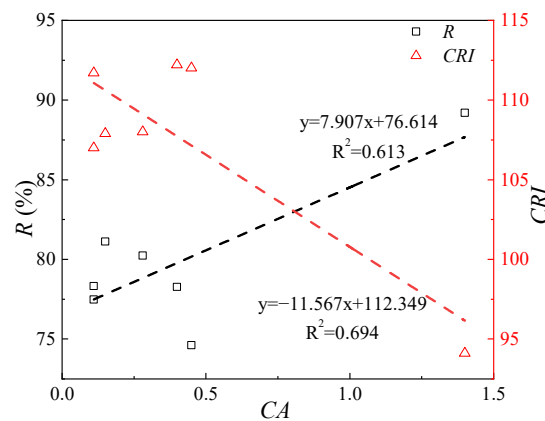


Figure 25. Correlation of CA with R and CRI .

The performance of the asphalt mixture was affected by the gradation, but the gradation range alone was not sufficient to determine the quality of the asphalt mixture. The results of different tests showed that different gradation ranges had different advantages and disadvantages in terms of flexural fatigue resistance, low-temperature cracking resistance, resistance to crack expansion, and deformation resistance. Therefore, to better characterize the performance of the asphalt mixture, the influencing factors and the optimal values of the gradation parameters need to be further analyzed, as shown in Table 6.

Table 6. Main gradation parameters of different test.

Gradation Parameters	$P_{4.75mm}$	$P_{2.36mm}$	$PCSI$	D_c	CA	Asphalt Film Thickness
BBT	✓	✓	✓	✓		
LT-SCB test						✓
CE-SCB test	✓	✓	✓	✓		
OT					✓	

The main influencing parameters of the asphalt mixture performance varied depending on the test method. The BBT and CE-SCB test were mainly influenced by the coarse aggregate passing rates, $PCSI$, and D_c , while the LT-SCB test was mainly influenced by the asphalt film thickness and the OT was mainly influenced by the CA. The increase in the coarse aggregate passing rates, $PCSI$, and D_c and the decrease in the 2.36 mm aggregate content improved the performance of the asphalt mixture in the BBT but reduced its performance in the CE-SCB test, suggesting that these two tests reflected different aspects of the asphalt mixture performance. The decrease in the asphalt film thickness enhanced the performance of the asphalt mixture in the LT-SCB, indicating that the asphalt film thickness was a key factor affecting the low-temperature cracking resistance of the asphalt mixture. The performance of the asphalt mixture in the OT improved with the decrease in the CA, which indicated that the CA was a significant parameter affecting the damage resistance of the asphalt mixture.

3.5. Relevance of Evaluation Methods

The crack resistance of asphalt mixtures is an important performance indicator, but there is a lack of a unified test method and evaluation standard for it. In this paper, four different tests were used to evaluate the crack resistance of asphalt mixtures under various conditions: the BBT, LT-SCB, CE-SCB, and OT tests. For a more comprehensive evaluation of the crack resistance of asphalt mixtures, the relationship and differences between these four tests need to be further investigated.

3.5.1. Dispersion of Tests

To evaluate the crack resistance of asphalt mixtures more effectively, this paper used the coefficient of variation as a measure of data dispersion. The coefficient of variation is the ratio of the standard deviation to the mean value. The lower the coefficient of variation, the more stable and reliable the parallel test data are. The higher the coefficient of variation, the more dispersed and uncertain the parallel test data are. This paper analyzed the coefficient of variation for the parallel test results of different tests, as shown in Figure 26.

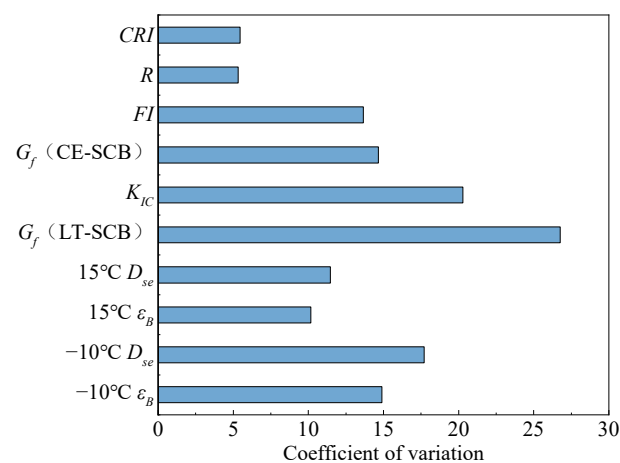


Figure 26. Coefficient of variation of parallel test.

The data dispersion of different tests varied significantly. The OT had the most stable data, with the lowest coefficient of variation values of 5.33 and 5.45, respectively. This indicated that the OT had high repeatability and reliability. The LT-SCB test had the most dispersed data, with the highest coefficient of variation value of 26.77. This indicated that the LT-SCB test was influenced by various factors.

3.5.2. Distinction of Tests

To analyze the ability of different tests to distinguish the gradation of asphalt mixtures, the coefficient of variation of the mean value of each test parameter under different gradation conditions was calculated, as shown in Figure 27. The coefficient of variation reflected the degree of variation of the parameter value under different gradations, and the higher the coefficient of variation, the higher the sensitivity of the parameter to gradation, and the better the ability to distinguish the effect of gradation on the performance of the asphalt mixture.

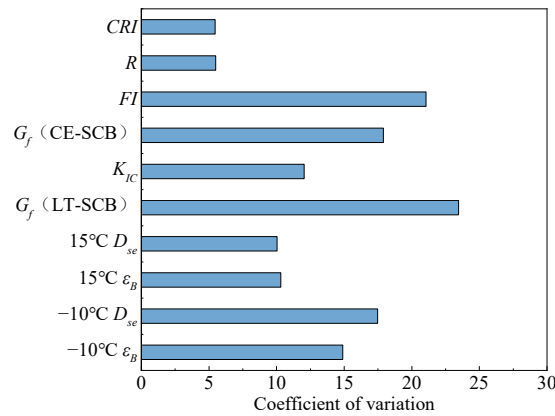


Figure 27. Coefficient of variation of test indicators.

The ability of different tests to differentiate the gradation of asphalt mixtures varied significantly. The LT-SCB test had the highest coefficient of variation value of 23.45, indicating that it was the most sensitive to gradation changes and could effectively distinguish the effects of different gradations on the performance of the asphalt mixture. The OT had the lowest coefficient of variation value of 5.47, indicating that it was the least sensitive to gradation changes and could not effectively distinguish the effects of different gradations on the performance of the asphalt mixture.

3.5.3. Correlation of Tests

To examine the correlation between different tests, the Pearson test was conducted. The Pearson test measures the linear correlation between data using a correlation coefficient that ranges from -1 to 1 . A correlation coefficient close to 1 or -1 indicates a strong correlation, while a correlation coefficient close to 0 indicates a weak correlation. The results of the Pearson correlation analysis are shown in Figure 28.

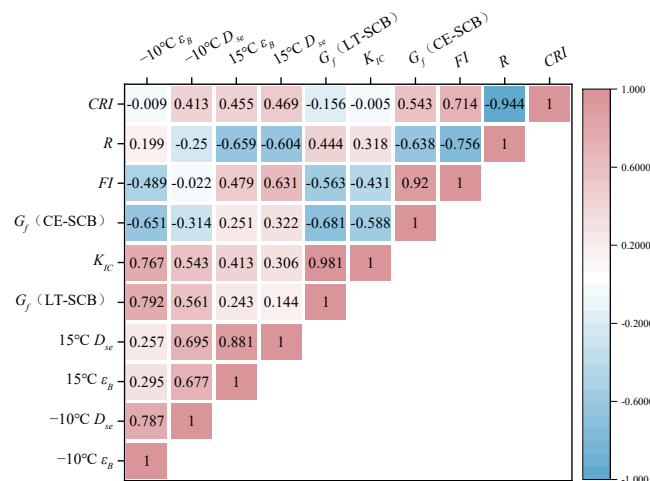


Figure 28. The results of the Pearson correlation analysis.

- (a) The $-10\text{ }^{\circ}\text{C}$ BBT had a good positive correlation with the LT-SCB test. The correlation coefficients between their parameters were all greater than 0.5, indicating that the flexural fatigue resistance and the low-temperature crack resistance of the asphalt mixture were consistent under low-temperature conditions. The higher the toughness of the asphalt mixture, the higher its deformation and load dissipation, and the higher its crack resistance.
- (b) The $15\text{ }^{\circ}\text{C}$ BBT had a poor correlation with other tests. The correlation coefficients between their parameters were mainly less than 0.5, indicating that the flexural fatigue resistance of the asphalt mixture at room temperature was different from other types of cracking resistance.
- (c) The CE-SCB test had a good correlation with the OT. The correlation coefficients between the G_f , FI , and the R and CRI were -0.638 , 0.543 , and -0.756 , 0.714 , respectively. These values indicated that the G_f of the asphalt mixture increased as the R decreased. The FI and CRI characterized the load decay and the crack growth rate after peak load. The higher the FI and CRI , the slower the load decay and the crack growth, and the higher the crack resistance.
- (d) The $-10\text{ }^{\circ}\text{C}$ BBT, LT-SCB, CE-SCB, and OT tests had some degree of negative correlation. For example, the correlation coefficient between the G_f of the LT-SCB test and the G_f of the CE-SCB test was -0.681 , which implies that the asphalt mixture with higher energy consumption at low-temperature cracking was less prone to cracking, while the asphalt mixture with lower energy consumption at crack expansion after cracking had faster crack development. This indicated that the cracking mechanism of asphalt mixtures under different conditions was different and that different types of tests should be considered comprehensively in performance evaluation.

In summary, the BBT, LT-SCB, CE-SCB, and OT tests can evaluate the crack resistance of asphalt mixtures, but they have different emphases. The LT-SCB test is highly influenced by the asphalt film thickness, which cannot effectively reflect the impact of gradation change on crack resistance. Moreover, the specimen preparation process is complex, time-consuming, and limited by equipment conditions. The OT data are relatively stable, but the test sensitivity to gradation is low. Therefore, this paper suggests that the ε_B and D_{sc} of the $-10\text{ }^{\circ}\text{C}$ BBT and the G_f and FI of the CE-SCB test should be used as the crack resistance evaluation indices of AR-SAMI.

4. Conclusions

In this paper, the influence of gradation on the stress absorption performance of AR-SAMI was studied. Based on the BBT, LT-SCB, CE-SCB, and OT tests, key sieve hole method, graded fractal method, and Bayley method parameters were used as indicators. The main conclusions are as follows:

- The AR-SAMI with different gradations showed different performance in different tests, with a maximum difference of 56.07%. The AR-SAMI of 10B gradation had the best performance in the BBT, while the AR-SAMI of 10A and 10B gradation had the best performance in the LT-SCB test. The AR-SAMI of 10C gradation had the best performance in the CE-SCB test, and the AR-SAMI of 10B and 10C gradation had good performance in the OT.
- The different tests were influenced by different parameters. The performance of the AR-SAMI in the BBT improved with the increase of the $P_{4.75\text{mm}}$ and $P_{2.36\text{mm}}$, $PCSI$, and D_c . However, the performance of the AR-SAMI in the CE-SCB test deteriorated with the increase of these parameters. The performance of the AR-SAMI in the LT-SCB test improved with the increase of the asphalt film thickness, while the performance of the AR-SAMI in the OT worsened with the increase of the CA .
- The stress absorption performance of asphalt mixtures consisted of two aspects: crack resistance and crack expansion resistance. These two aspects were inversely related to each other, meaning that a mixture with better crack resistance did not necessarily have better crack expansion resistance.

- The $-10\text{ }^{\circ}\text{C}$ BBT, LT-SCB, CE-SCB, and OT tests could be used to evaluate the stress absorption performance, but they reflected different aspects of performance. It was recommended to use the $-10\text{ }^{\circ}\text{C}$ BBT and CE-SCB tests as the evaluation methods of stress absorption performance. The ε_B and D_{se} of the $-10\text{ }^{\circ}\text{C}$ BBT and the G_f and FI of the CE-SCB test were recommended as the evaluation indicators.

This paper evaluated the stress absorption performance of asphalt mixtures with different gradations, but the number of gradations was limited, and, thus, could not provide a comprehensive and effective comparison. Therefore, further research is needed to explore the influence of more gradations on stress absorption performance. In addition, this paper only focused on the effect of gradation on stress absorption, which was not sufficient to reflect the actual engineering performance of asphalt mixtures. It is recommended to combine the road performance of AR-SAMI with the stress absorption performance to obtain a more realistic and comprehensive evaluation.

Author Contributions: Conceptualization, P.L.; methodology, P.L.; validation, X.X.; formal analysis, X.X.; investigation, S.T.; resources, P.L.; data curation, J.L.; writing—original draft preparation, X.X.; writing—review and editing, W.P.; visualization, B.W.; supervision, S.L.; project administration, P.L.; funding acquisition, P.L. All authors have read and agreed to the published version of the manuscript.

Funding: This research was funded by the National Key Research and Development Program of China, grant number 2021YFB2601000, Guangxi Key Research and Development Program, grant number AB21220070, Guangxi Science and Technology Major Program, grant number 2023AA14005, and Airport Engineering Research Center of CAAC Program, grant number ERCAOTP20220301.

Institutional Review Board Statement: Not applicable.

Informed Consent Statement: Not applicable.

Data Availability Statement: Not applicable.

Conflicts of Interest: The authors declare no conflict of interest.

References

1. Oshone, M.; Dave, E.V.; Sias, J.E. Asphalt mix fracture energy based reflective cracking performance criteria for overlay mix selection and design for pavements in cold climates. *Constr. Build. Mater.* **2019**, *211*, 1025–1033. [[CrossRef](#)]
2. Wang, X.; Zhong, Y. Reflective crack in semi-rigid base asphalt pavement under temperature-traffic coupled dynamics using XFEM. *Constr. Build. Mater.* **2019**, *214*, 280–289. [[CrossRef](#)]
3. Idris, I.I.; Sadek, H.; Hassan, M. State-of-the-Art Review of the Evaluation of Asphalt Mixtures' Resistance to Reflective Cracking in Laboratory. *J. Mater. Civ. Eng.* **2020**, *32*, 3120004. [[CrossRef](#)]
4. Rith, M.; Lee, S.W. Development of cohesive-zone-based prediction model for reflective cracking in asphalt overlay. *Int. J. Pavement Eng.* **2022**, *23*, 1050–1059. [[CrossRef](#)]
5. Zeng, Z.; Guo, Y.; Li, P.; Shen, A.; Zhai, C. Performance research of fiber-reinforced asphalt rubber as a stress-absorbing membrane interlayer. *J. Adhes. Sci. Technol.* **2021**, *35*, 2047–2063. [[CrossRef](#)]
6. Zhang, K.; Zhang, Z.; Luo, Y. Material Composition Design and Anticracking Performance Evaluation of Asphalt Rubber Stress-Absorbing Membrane Interlayer (AR-SAMI). *Hindawi* **2018**, *2018*, 8560604. [[CrossRef](#)]
7. Chen, Y.; Lopp, G.; Roque, R. Effects of an Asphalt Rubber Membrane Interlayer on Pavement Reflective Cracking Performance. *J. Mater. Civ. Eng.* **2013**, *25*, 1936–1940. [[CrossRef](#)]
8. Wargo, A.; Safavizadeh, S.A.; Kim, Y.R. Comparing the Performance of Fiberglass Grid with Composite Interlayer Systems in Asphalt Concrete. *Transp. Res. Record* **2017**, *2631*, 123–132. [[CrossRef](#)]
9. Deng, H.L.; Fu, X.Y.; Gao, W.X.; Ni, T.T.; Chen, K.J. Research on New Technology to Control Highway Semi-Rigid Base Asphalt Pavement Cracks. *Adv. Mater. Res.* **2011**, *194*, 1632–1638. [[CrossRef](#)]
10. Ogundipe, O.M.; Thom, N.; Collop, A. Investigation of crack resistance potential of stress absorbing membrane interlayers (SAMIs) under traffic loading. *Constr. Build. Mater.* **2013**, *38*, 658–666. [[CrossRef](#)]
11. Ogundipe, O.M.; Thom, N.H.; Collop, A.C. Evaluation of performance of stress-absorbing membrane interlayer (SAMI) using accelerated pavement testing. *Int. J. Pavement Eng.* **2013**, *14*, 569–578. [[CrossRef](#)]
12. Li, Z.Z.; Chen, S.F.; Liao, W.D.; Yuan, R.X. Lab Simulation Study on Anti-Cracking Performance of Asphalt Concrete Overlays for Fatigue. *Adv. Mater. Res.* **2012**, *510*, 478–483. [[CrossRef](#)]
13. Pan, R.; Li, Y. Effect of warm mix rubber modified asphalt mixture as stress absorbing layer on anti-crack performance in cold region. *Constr. Build. Mater.* **2020**, *251*, 118985. [[CrossRef](#)]

14. Baghel, R.S.; Kasu, S.R.; Chandrappa, A.K. Effect of dual and new generation wide-base tire assembly on inverted pavements. *J. Road Eng.* **2022**, *2*, 124–136. [[CrossRef](#)]
15. Yu, B.; Lu, Q.; Yang, J. Evaluation of anti-reflective cracking measures by laboratory test. *Int. J. Pavement Eng.* **2013**, *14*, 553–560. [[CrossRef](#)]
16. Asadi, S.; Shafabakhsh, G. Experimental and statistical investigation on the performance of asphalt overlays reinforced with geocomposite in controlling the reflective cracks under different loadings and temperatures. *SN Appl. Sci.* **2023**, *5*, 202. [[CrossRef](#)]
17. Shafabakhsh, G.; Ahmadi, S. Reflective cracking reduction by a comparison between modifying asphalt overlay and sand asphalt interlayer: An experimental evaluation. *Int. J. Pavement Eng.* **2021**, *22*, 192–200. [[CrossRef](#)]
18. Zhang, Q. Effect of Grading Type on the Performance of Warm-Mix Rubber-Asphalt Mixture. *IOP Conf. Ser. Earth Environ. Sci.* **2020**, *526*, 12152. [[CrossRef](#)]
19. Tran, N.T.; Takahashi, O. Effect of aggregate gradation on the cracking performance of wearing course mixtures. *Constr. Build. Mater.* **2017**, *152*, 520–528. [[CrossRef](#)]
20. Germann, F.P.; Lytton, R.L. *Methodology for Predicting the Reflection Cracking Life of Asphalt Concrete Overlays*; Report No. 207-5; Texas State Department of Highways and Public Transportation: Austin, TX, USA, 1979.
21. Zhou, F.; Hu, S.; Chen, D.H.; Scullion, T. Overlay Tester: Simple Performance Test for Fatigue Cracking. *Transp. Res. Rec. J. Transp. Res. Board* **2007**, *2001*, 1–8. [[CrossRef](#)]
22. Wang, S.; Yan, K.; Ge, D.; Hong, Z. Laboratory research on the performance of stress-absorption interlayer (SAI) of waste tire rubber and amorphous poly alpha olefin modified asphalt. *Constr. Build. Mater.* **2019**, *223*, 830–840. [[CrossRef](#)]
23. Liu, J.Y.; Zhang, L.J.; Kou, B.; Shen, P. The Environment-Friendly High-Elasticity Asphalt Mixture Using as Stress Absorbing Layer. *Adv. Mater. Res.* **2012**, *490*, 3753–3761. [[CrossRef](#)]
24. Zhou, F.; Newcomb, D.; Gurganus, C.; Banihashemrad, S.; Park, E.S.; Sakhaeifaran, M.; Lytton, R.L. *Experimental Design for Field Validation of Laboratory Tests to Assess Cracking Resistance of Asphalt Mixtures*; NCHRP Final Report 9-57; Transportation Research Board National Research Council: Washington, WA, USA, 2016; p. 103.
25. CJJ/T273-2019; Rubber Asphalt Pavement Technical Standard. Ministry of Housing and Urban Rural Development of the People's Republic of China: Beijing, China, 2019.
26. JT/T 798-2011; Asphalt Rubber for Highway Engineering. Ministry of Transport of the People's Republic of China: Beijing, China, 2011.
27. JTG E20-2011; Standard Test Methods of Bitumen and Bituminous Mixtures for Highway Engineering. Ministry of Transport of the People's Republic of China: Beijing, China, 2011.
28. JTG F40-2004I; Technical Specifications for Construction of Highway Asphalt Pavement. Ministry of Transport of the People's Republic of China: Beijing, China, 2004.
29. Bischoff, D.L. *Evaluation of Strata[®] Reflective Crack Relief System*; Cost Effectiveness; Wisconsin Department of Transportation, Division of Transportation Systems Development, Bureau of Technical Services, Materials Management Section: Madison, WI, USA, 2007.
30. Blomberg, J.M. Superpave Overlay of Sand Anti-Fracture Layer Over PCCP. In *Concrete Pavements*; Department of Transportation: Jefferson City, MO, USA, 2000.
31. Scullion, T. *Technical Bulletin on Design and Construction of Crack Attenuating Mixes (CAM)*; Texas Transportation Institute: College Station, TX, USA, 2010.
32. DB45/T 1098-2014; Technical Specification for Construction of Asphalt Rubber Pavement. Guangxi Zhuang Autonomous Region Bureau: Nanning, China, 2014.
33. DB 36/T 744-2013; Technical Specifications for Waste Tire Rubber Asphalt Pavement Construction. Jiangxi Provincial Bureau of Quality and Technical Supervision: Nanchang, China, 2013.
34. DG/TJ08-2109-2012; Technical Code for Asphalt Rubber Pavement. Shanghai Urban-Rural Construction and Transportation Commission: Shanghai, China, 2012.
35. DB11/T 916-2012; Technical specifications for asphalt rubber. Beijing Municipal Bureau of Quality and Technical Supervision: Beijing, China, 2012.
36. DB13/T 1013-2009; Technical standard for tire crumb asphalt rubber and asphalt rubber hot mixture. Hebei Provincial Bureau of Quality and Technical Supervision: Shijiazhuang, China, 2009.
37. DB 14/T 160-2015; Technical specification for highway modified asphalt pavement construction. Shanxi Provincial Bureau of Quality and Technical Supervision: Taiyuan, China, 2015.
38. DBJ/T13-147-2012; Specification for Construction Technology of Stabilized Rubber Modified Asphalt Pavement. Fujian Provincial Department of Housing and Urban Rural Development: Fuzhou, China, 2012.
39. Leiva, F.; West, R.C. *Using the Primary Control Sieve Index to Define Gradation Type and as a Factor Related to Asphalt Mixture Properties*; National Center for Asphalt Technology: Auburn, AL, USA, 2021.
40. AASHTO TP 105-13; Standard Method of Test for Determining the Fracture Energy of Asphalt Mixtures Using the Semicircular Bend Geometry (SCB). American Association of State Highway and Transportation Officials: Washington, DC, USA, 2019; p. 13.
41. EN 12697-44; Bituminous Mixtures-Test Methods for Hot Mix Asphalt-Part 44: Crack Propagation by Semi-Circular Bending Test. NSAI: Dublin, Ireland, 2010.

42. *AASHTO TP 124-16*; Standard Method of Test for Determining the Fracture Potential of Asphalt Mixtures Using Semicircular Bend Geometry (SCB) at Intermediate Temperature. American Association of State Highway and Transportation Officials: Washington, DC, USA, 2016.
43. *Tex-248-F*; Texas Department of Transportation Test Procedure for Overlay Test. Texas Department of Transportation: Austin, TX, USA, 2017; pp. 1–13.

Disclaimer/Publisher's Note: The statements, opinions and data contained in all publications are solely those of the individual author(s) and contributor(s) and not of MDPI and/or the editor(s). MDPI and/or the editor(s) disclaim responsibility for any injury to people or property resulting from any ideas, methods, instructions or products referred to in the content.